

REPORT DOCUMENTATION PAGE				Form Approved OMB No. 0704-0188	
Public reporting burden for this collection of information is estimated to average 1 hour per response, including the time for reviewing instructions, searching existing data sources, gathering and maintaining the data needed, and completing and reviewing this collection of information. Send comments regarding this burden estimate or any other aspect of this collection of information, including suggestions for reducing this burden to Department of Defense, Washington Headquarters Services, Directorate for Information Operations and Reports (0704-0188), 1215 Jefferson Davis Highway, Suite 1204, Arlington, VA 22202-4302. Respondents should be aware that notwithstanding any other provision of law, no person shall be subject to any penalty for failing to comply with a collection of information if it does not display a currently valid OMB control number. <b>PLEASE DO NOT RETURN YOUR FORM TO THE ABOVE ADDRESS.</b>					
1. REPORT DATE (DD-MM-YYYY) 14-02-2011		2. REPORT TYPE Journal Article		3. DATES COVERED (From - To)	
4. TITLE AND SUBTITLE  Structure and Dynamics of the 1-Hydroxyethyl-4-amino-1,2,4-triazolium Nitrate (HEATN) High Energy Ionic Liquid System (Preprint)				5a. CONTRACT NUMBER	
				5b. GRANT NUMBER	
				5c. PROGRAM ELEMENT NUMBER	
6. AUTHOR(S) Philip J. Carlson (Iowa State University), Sayantan Bose (Iowa State University), Daniel W. Armstrong (Univ. of Texas), Tommy Hawkins (AFRL/RZSP), Mark S. Gordon (Iowa State University), and Jacob W. Petrich (Iowa State University)				5d. PROJECT NUMBER	
				5f. WORK UNIT NUMBER 23030423	
7. PERFORMING ORGANIZATION NAME(S) AND ADDRESS(ES)  Iowa State University Ames Laboratory and Department of Chemistry Ames, Iowa 50011				8. PERFORMING ORGANIZATION REPORT NUMBER  AFRL-RZ-ED-JA-2011-032	
9. SPONSORING / MONITORING AGENCY NAME(S) AND ADDRESS(ES)  Air Force Research Laboratory (AFMC) AFRL/RZS 5 Pollux Drive Edwards AFB CA 93524-7048				10. SPONSOR/MONITOR'S ACRONYM(S)	
				11. SPONSOR/MONITOR'S NUMBER(S) AFRL-RZ-ED-JA-2011-032	
12. DISTRIBUTION / AVAILABILITY STATEMENT  Approved for public release; distribution unlimited (PA #10781).					
13. SUPPLEMENTARY NOTES For publication in Journal of Physical Chemistry A, July 2011					
14. ABSTRACT We have undertaken an investigation of the structure and dynamics of the high-energy ionic liquid, 1-hydroxyethyl-4-amino-1,2,4-triazolium nitrate (HEATN). Both experimental and computational methods have been employed to understand the fundamental properties, characteristics, and behavior of HEATN. This system maintains an even charge separation, as assessed by both the Mulliken and geodesic derived charges, in contrast to other reports on triazolium ionic liquids. The MP2 level optimizations find six dimer and five tetramer structures and show the significant highly hydrogen bonded network within HEATN. The fragment molecular orbital (FMO) method adequately treats this ionic liquid system as evidenced by the small relative error obtained while avoiding the prohibitive scaling of other ab initio electronic structure methods. The solvation dynamics of the HEATN system were investigated via the coumarin 153 probe at five different temperatures, and the rotational dynamics were measured. Comparisons with previously studied imidazolium and phosphonium ionic liquids show surprising similarity. To our knowledge, this the first study of solvation dynamics in a triazolium based ionic liquid.					
15. SUBJECT TERMS					
16. SECURITY CLASSIFICATION OF:			17. LIMITATION OF ABSTRACT	18. NUMBER OF PAGES	19a. NAME OF RESPONSIBLE PERSON
a. REPORT	b. ABSTRACT	c. THIS PAGE			Mr. Wayne Kalliomaa
Unclassified	Unclassified	Unclassified	SAR	42	19b. TELEPHONE NUMBER (include area code) N/A

# Structure and Dynamics of the 1-Hydroxyethyl-4-amino-1,2,4-triazolium Nitrate (HEATN) High Energy Ionic Liquid System

*Philip J. Carlson,<sup>†</sup> Sayantan Bose,<sup>†</sup> Daniel W. Armstrong,<sup>‡</sup> Tommy Hawkins,<sup>§</sup>*

*Mark S. Gordon,<sup>†\*</sup> and Jacob W. Petrich<sup>†\*</sup>*

<sup>†</sup> Ames Laboratory and Department of Chemistry, Iowa State University, Ames, Iowa 50011

<sup>‡</sup> Department of Chemistry and Biochemistry, University of Texas, Arlington, Box 19065

Arlington, Texas 76019

<sup>§</sup> Air Force Research Laboratory, 10 East Saturn Boulevard, Building 8451, Edwards Air Force Base,  
California 93524

\* To whom correspondence should be addressed. Email: mgordon@iastate.edu, jwp@iastate.edu

Distribution A: Approved for public release; distribution unlimited

## Abstract

We have undertaken an investigation of the structure and dynamics of the high-energy ionic liquid, 1-hydroxyethyl-4-amino-1,2,4-triazolium nitrate (HEATN). Both experimental and computational methods have been employed to understand the fundamental properties, characteristics, and behavior of HEATN. This system maintains an even charge separation, as assessed by both the Mulliken and geodesic derived charges, in contrast to other reports on triazolium ionic liquids. The MP2 level optimizations find six dimer and five tetramer structures and show the significant highly hydrogen bonded network within HEATN. The fragment molecular orbital (FMO) method adequately treats this ionic liquid system as evidenced by the small relative error obtained while avoiding the prohibitive scaling of other *ab initio* electronic structure methods. The solvation dynamics of the HEATN system were investigated via the coumarin 153 probe at five different temperatures, and the rotational dynamics were measured. Comparisons with previously studied imidazolium and phosphonium ionic liquids show surprising similarity. To our knowledge, this the first study of solvation dynamics in a triazolium based ionic liquid.

## Introduction

There has been a steeper than exponential growth in the number of publications related to ionic liquids since the year 2000.<sup>1</sup> The interest in ionic liquids is undoubtedly owing to the environmentally friendly nature of these compounds.<sup>2-4</sup> Ionic liquids can be liquid at room temperature and are molten salts commonly composed of an organic cation and an inorganic anion. These low-melting salts are considered green solvents, in contrast to volatile organic compounds (VOCs), due to their high chemical and thermal stabilities, negligible vapor pressure,<sup>5</sup> and high recoverability and reusability.<sup>6,7</sup> Ionic liquids can be customized by varying the identity of the substituents on the cation or adapting the moiety of the anion.<sup>8</sup> This versatility and these unique properties have piqued the interest of the scientific community, and a variety of fundamental studies<sup>9-15</sup> have been performed on them to obtain a better understanding of their characteristics.

One interesting application of ionic liquids is in the high energy density materials (HEDM) community where many different molten salts have been explored and reported.<sup>16</sup> It is important to understand what characteristics make ionic liquids suited to HEDM applications. This very problem was explored computationally in a series of studies,<sup>17-19</sup> as well as experimentally in a few reports.<sup>20</sup> These studies show that triazolium ionic liquids appear to have more suitable characteristics for HEDM application than other nitrogen rich ionic liquid species.

A recent report by Drake and co-workers<sup>21</sup> on low-melting, potentially energetic, salts lists the desired characteristics for these salts, as well as potential benefits that might be derived from using them in energetic materials applications. The same authors have discussed the 1-R-4-amino-1,2,4-triazolium family of salts<sup>22</sup> that are of interest owing to their high nitrogen content. One interesting room temperature ionic liquid in this family is 1-hydroxyethyl-4-amino-1,2,4-triazolium nitrate (HEATN), depicted in **Figure 1**. To use this ionic liquid in various applications it is beneficial to employ both experimental and computational methods to understand its fundamental properties, characteristics, and behavior.

This present work focuses on the physical chemistry of the high-energy ionic liquid system HEATN. The HEATN system was recently investigated using molecular dynamics simulations for prediction of bulk properties.<sup>23</sup> The studies presented here assess this ionic liquid at a molecular level, by using *ab initio* electronic structure methods, to gain insight into the structure, energetics and charge delocalization in the component ions. These properties have been shown to be of significance in relation to the physical and chemical properties of ionic liquids,<sup>24</sup> and *ab initio* electronic structure methods have been shown to give excellent agreement with X-ray structures of triazole salts giving bond lengths within 0.003 nm of the experimental values in the case of the common 3,4,5-triamino-1,2,3-triazole salts.<sup>25</sup> Performing electronic structure calculations on large systems of ionic liquids can be difficult given the fact that *ab initio* electronic structure theory methods scale  $\sim N^4$  or worse, depending on the chosen method and if electron correlation is included, where N measures the size of the system. This means that correlated electronic structure methods become computationally prohibitive for very large systems with more than 100 heavy atoms. A typical approach for large systems is to treat sections of higher interest using quantum mechanics (QM) and other section using molecular mechanics (MM). These combined QM/MM methods have had some success for large systems yet at times important contributions from parts of the system may be treated by classical model potentials having a significant impact on the QM region leading to the sacrificing of high accuracy to save time and resources. Alternatively, breaking the large system up into smaller sections and treating these fragments with particular levels of electronic structure theory has the advantage of being virtually fully quantum mechanical. Fragmentation methods have a number of distinct advantages without losing accuracy for larger systems.<sup>26,27</sup> The fragment molecular orbital (FMO) method<sup>27-31</sup> splits the system up into fragments and computes each fragment (monomer) in the electrostatic potential of the other fragments. The FMO method is suited for larger systems and has been applied to systems such as polypeptides and proteins,<sup>32</sup> and even a heavy metal system containing 3596 atoms.<sup>33</sup> Large systems can be treated at a

high level of theory allowing valuable insight into large systems of ionic liquids. The use of the FMO method with ionic liquid systems has been limited and is explored in this report.

Additional studies used to investigate the HEATN system and its dynamics include the use of fluorescence spectroscopy to compare this high-energy ionic liquid to other more commonly used ionic liquids. Steady-state and time-resolved fluorescence measurements were performed to assess how HEATN behaves as a solvent at short time scales. In particular, solvation dynamics experiments were carried out using the fluorescent probe coumarin 153 (C153) in HEATN. The structure of C153 is given in **Figure 1**. C153 is an ideal probe, and has been used extensively in a large number of solvation dynamics studies in various media.<sup>34-50</sup> This permits facile comparison of the HEATN ionic liquid with other systems. A summary of the various solvation dynamics studies in ionic liquids has recently been published<sup>51</sup> as well a report with some of the applications of such explorations.<sup>52</sup> Up till now there have been no explorations of the solvation dynamics of triazolium ionic liquid systems. The solvation dynamics of the HEATN system were investigated via the C153 probe at five different temperatures, and the rotational dynamics were measured by exploiting the anisotropic nature of the probe's fluorescence through this viscous ionic liquid and comparisons with previously studied imidazolium and phosphonium ionic liquids are presented.

## **Materials and Methods**

### **Computational methods.**

Molecular structures were obtained by performing geometry optimization calculations using second-order Moller-Plesset perturbation theory (MP2)<sup>53</sup> with a Hartree-Fock reference. All calculations were made using the 6-31++G(d,p) Pople type basis set. Hessians (matrices of the second derivatives of the energies) were determined to ensure each stationary point was truly a minimum or a transition state. Population analysis was completed using Mulliken's method<sup>54-57</sup> and geodesic derived charges.<sup>58</sup> Studies of three cation-anion pairs (hexamers) were carried out using the FMO method.<sup>28</sup> The fragment molecular orbital method provides a way of treating large systems with high accuracy by overcoming

the prohibitive scaling associated with *ab initio* electronic structure theory methods. This is accomplished by dividing the large molecular system of interest into fragments (each called monomers) and executing the now feasible *ab initio* calculations on the fragments and their interaction with another fragment (dimers) or two other fragments (trimers) in the presence of the other monomers.<sup>29</sup> Such that the total energy of a fragmented dimer system is given as follows:  $E = \sum_I^N E_I + \sum_{I>J}^N (E_{IJ} - E_I - E_J)$ , where the energy ( $E$ ) is given by the standard SCF method for each monomer ( $I$ ) for a total of  $N$  fragments in the electrostatic field of the additional  $N-1$  fragments, and dimer ( $IJ$ ) calculated in the electrostatic field of the other  $N-2$  fragments. The FMO method has been enhanced by the use of the generalized distributed data interface (GDDI) allowing two levels of parallelization,<sup>59</sup> and is available in a multilevel format allowing one to assign fragments to particular levels so that you can treat these different levels with different electronic structure methods and/or basis sets.<sup>60</sup> With this ionic liquid system one molecular ion was assigned to a fragment, thereby removing the need to fragment bonds as is common with large covalently bonded systems. For covalently bonded systems there are some guidelines that can help to obtain the best level of accuracy.<sup>28</sup> The FMO calculations were carried out using the two-body correction in conjunction with MP2 (FMO2-MP2) as well as the three-body correction with MP2 (FMO3-MP2). All calculations were performed using GAMESS,<sup>61,62</sup> and were visualized when possible with MacMolPlt.<sup>63</sup>

## Materials.

Coumarin 153 (C153) (Exciton Inc., Dayton, OH) was used as received. 4-amino-1,2,4-triazole was purchased from Sigma. The production of 1-substituted-4-amino-1,2,4-triazolium nitrate ionic liquid molecules through a metathesis of heterocyclic halide and nitrate salts is well established.<sup>22,64</sup> The specific synthesis of 1-hydroxyethyl-4-amino-1,2,4-triazolium bromide (HEATB) and 1-hydroxyethyl-4-amino-1,2,4-triazolium nitrate (HEATN) from metathesis of HEATB with silver nitrate follows the procedure described by Drake, Hawkins and Tollison.<sup>65</sup>

The synthesis of the other ionic liquids shown in **Figure 1** is described elsewhere<sup>10</sup> and were decolorized according to the procedure described elsewhere.<sup>66</sup> Briefly, the impure ionic liquid was diluted and was allowed to elute through a column packed with celite, silica gel and activated charcoal. After the excess solvent was removed, the ionic liquid was dried under vacuum with mild heating. The water content of the HEATN sample was determined using a Mettler Toledo DL 39 coulometric Karl Fischer titrator. The viscosity of the HEATN sample was measured at each of the five temperatures  $\pm$  0.1 °C using a ViscoLab 4000 viscometer from Cambridge Applied Systems.

### **Steady-state measurements.**

Steady-state absorption spectra were obtained using a Hewlett-Packard 8453 UV-visible spectrophotometer with 1-nm resolution. Steady-state fluorescence measurements were taken using a SPEX fluormax-4 spectrofluorometer (HORIBA Jobin Yvon) with 1-nm resolution. The emission spectra were corrected for detector response and the lamp spectral intensity. All emission spectra were obtained with an excitation wavelength of 407 nm and a 3 nm band-pass. A 3 mm path length quartz cuvette was used for all measurements.

### **Time-resolved measurements.**

Fluorescence lifetime measurements were made using the time-correlated single-photon counting (TCSPC) apparatus described previously<sup>9,50</sup> a summary is included here. Using a home-made mode-locked Ti:sapphire oscillator pumped at 532 nm by a Nd:VO<sub>4</sub> Millennia (Spectra-Physics) laser femtosecond pulses were produced which were tunable from 780 nm – 900 nm having a repetition rate of 82 MHz. With the output selected at 814 nm from the Ti:Sapphire oscillator, the repetition rate was reduced to 8.8 MHz via the use of a Pockels cell (model 350-160 from Conoptics Inc.) and was subsequently frequency doubled through the use of a harmonic generator (model TP-2000B from U-Oplaz Technologies). The produced blue light having a wavelength of 407 nm was used as the primary excitation source for all time-resolved studies. After the harmonic generator a half-wave plate was



placed in front of a vertical polarizer to ensure the polarization of the excitation light. The fluorescence was collected at a 90° angle to the excitation source and then passed through an emission polarizer set to the magic angle (54.7°) with respect to the vertical excitation light. In the case of the anisotropy studies this polarizer was set to 0° and 90° with respect to the vertical excitation light respectively. A 425 nm cut-off filter was placed before a multichannel plate (MCP) (Hamanatsu) to help remove any unwanted scattered excitation light. When performing the solvation dynamics studies, a monochromator was placed before the MCP to ensure the collection at each selected wavelength. The signal from the MCP detector was amplified and sent to a Becker & Hickl photon counting module (model SPC-630). The instrument response function had a full width at half maximum (FWHM) of ~45 - 50 ps. The parallel and perpendicular-polarized fluorescence anisotropy decay curves were collected in a 22 ns time-window and fitted simultaneously following the method described by Cross and Fleming.<sup>67</sup> This method takes full advantage of the statistical properties of the measured curves. The solvation dynamics studies involved recording fifteen single wavelength decays from 490 nm to 630 nm in 10 nm intervals, in a time-window of 9 ns. Typically, 1024 channels of data were collected with 65,000 counts in the peak channel. The wavelength-resolved fluorescence transients were fit to sums of exponentials (typically 2 or 3, as necessary to fit the data), and time-resolved emission spectra (TRES) were reconstructed as described in previous reports.<sup>9,50</sup>

The traditional approach of fitting the time-resolved emission spectra to a log-normal function,<sup>9,34,68</sup> from which we extract the peak frequency  $\nu(t)$  as a function of time was used. The solvation dynamics is described by the following normalized correlation function:

$$C(t) = \frac{\nu(t) - \nu(\infty)}{\nu(0) - \nu(\infty)} \quad (1)$$

Because  $C(t)$  is a *normalized* function, the accurate determination of  $C(t)$  depends upon accurate values for  $\nu(0)$  and  $\nu(\infty)$ .  $\nu(0)$  is the frequency at zero-time, estimated using the method of Fee and Maroncelli,<sup>69</sup> who have described a robust, model independent, and simple procedure for generating this

Distribution A: Approved for public release; distribution unlimited

“zero-time” spectrum,  $\nu(0)$  which represents the emission spectrum expected prior to any solvent relaxation but after complete intramolecular vibrational redistribution. The validity has been checked using a different method for estimating the “zero-time” reorganization energy in a previous report.<sup>10</sup>  $\nu(\infty)$  is (usually<sup>70,71</sup>) the frequency at infinite time, obtained from the maximum of the steady state spectrum. (This is not, however, true in the case of very slowly relaxing solvents, as has been demonstrated in the case of certain ionic liquids<sup>12,70,71</sup>: where the emission spectrum at  $\sim 3$  times the fluorescence lifetime of the probe is *red-shifted* to that of the equilibrium spectrum.) The  $\nu(t)$ s are determined from the maxima of the log-normal fits of the time resolved emission spectra. In most of the cases, however, the spectra are broad, so there is some uncertainty in the exact position of the emission maxima. Thus, the range of the raw data points in the neighborhood of the maximum to estimate an error for the maximum obtained from the log-normal fit was considered. Depending on the width of the spectrum (i.e., “zero-time”, steady-state, or time-resolved emission spectrum), it was determined that the typical uncertainties are as follows: “zero-time”  $\sim$  steady-state ( $\sim \pm 100 \text{ cm}^{-1}$ )  $<$  time-resolved emission ( $\sim \pm 200 \text{ cm}^{-1}$ ). These uncertainties were used to compute error bars for the  $C(t)$  graph (giving maximum error of  $\pm 0.04$ ). Finally, in generating the  $C(t)$  curve, the first point was obtained from the “zero-time” spectrum. The second point was taken at the maximum of the instrument response function. The fractional solvation was also computed at 50 ps by taking  $f_{50ps} = 1 - C(t=50ps)$ . The experiments were also carried out at five different temperatures (25 °C, 35 °C, 45 °C, 55 °C and 65 °C) that were obtained using a variable temperature sample cell holder.

## Results and Discussion

**HEATN Structures.** A previous *ab initio* investigation<sup>17</sup> of triazolium ionic liquid systems showed a tendency for proton transfer between the cation and the anion to form neutral pairs. This tendency was investigated within the HEATN system by performing geometry optimizations on the different pairs of cations and anions. The geometric structures of both single cation-anion pairs (dimers) and two cation-anion pairs (tetramers) have been investigated. Six structures labeled I, II, III, IV, V, and

Distribution A: Approved for public release; distribution unlimited

VI were found for the HEATN dimer (**Table 1**) at the MP2 level. They are ordered with respect to their relative energies with structure “I” having the lowest energy. The relative energies can be seen in **Table 1** along with the hydrogen bond distances, Mulliken charges, and geodesic derived charges. The charge delocalization of each of these systems shows a very even charge separation between the cation and the anion as expected. Typically the geodesic charges are considered to be superior to the Mulliken charges; yet good agreement between these two methods is seen in most of these cases. Each of these structures show two hydrogen bonds between the cation and anion giving evidence that the HEATN system is a highly hydrogen bonded system. This is in part by design, as this liquid was chosen due to its potential as a perspective fuel. Having a higher density, which the hydrogen bonds may contribute to, is one of the desirable properties of high energy materials as this allows more energy per cubic centimeter. Since no geometries were found where the anion is to the side of the cation it seems that the hydroxyethyl side chain on the cation allows for the carousal of the nitrate anion.

In addition, the HEATN system was investigated at the tetramer (four molecules) level using the MP2 method. The geometries obtained can be seen in **Figure 2**. The relative energies, hydrogen bond distances, and both the Mulliken and geodesic charges are given in **Table 2**. Interestingly, these structures show less sharing of the anions between the cations. The cations seem to prefer to interact with only one anion and are correlated via hydrogen bonds to only a single anion. The charge separation is very even in the lowest energy structure found while the other structures show a less even distribution.

The FMO method was used to evaluate its feasibility for use with larger (hexamer and higher) charged ionic systems such as this ionic liquid. These structures serve as a great reference point to explore how both the FMO2-MP2 and the FMO3-MP2 method handle this highly energetic ionic liquid system. Applying these FMO methods to the MP2 geometries yields the results as seen in **Table 3**. As expected, the three-body correction (FMO3-MP2) does a better job of recovering the MP2 results. Comparing the results from the FMO2 and FMO3 methods it is immediately seen that they both recover

the MP2 energy well with the largest absolute difference being  $< 1$  kcal/mol in the FMO2 case and  $< 0.30$  kcal/mol using the FMO3 method. While in general better results are obtained using the three-body correction it is often not employed with smaller systems because of the additional computer time and resources required. In this particular case the MP2 method used 71.55 MB of RAM while the FMO2-MP2 and FMO3-MP2 methods used 5.07 MB and 11.47 MB respectively. It seems that as the system grows the extra cost of using the FMO3-MP2 method will be outweighed by the more accurate results obtained.<sup>26</sup> The charges found using both the Mulliken and geodesic charge schemes derived from the FMO2 and FMO3 single point calculations show good agreement to those found as derived from the MP2 method. The geodesic charges show that there is an acceptable treatment of the charges by the Mulliken scheme, at least in the case of this ionic liquid.

The accuracy using the FMO methods can be increased by making a few different changes. Larger systems can be more accurately (in comparison to the MP2 results) calculated by including more molecules per fragment. This would increase the costs of such calculations but very large systems can achieve additional accuracy this way. Fragment methods must normally be tailored to specific applications to achieve higher accuracy. That is, particular schemes of how many molecules per fragment and how to divide molecules into fragments may vary for different systems. More work needs to be done on larger systems of HEATN molecules to determine how exactly the HEATN system should be partitioned into fragments to achieve the most reasonable level of accuracy for large systems of HEATN.

### **Solvation Dynamics of C153 in HEATN**

HEATN was investigated using the fluorescent probe molecule C153. The maximum of the emission spectrum maximum is at 546 nm and is typical of C153 in other solvents. There was no temperature dependent shift of the absorption and emission spectra of C153 in HEATN. In order to construct the solvation correlation function  $C(t)$ , time-resolved fluorescence decays were collected at different wavelengths spanning the entire range of the emission spectrum of the probe as shown in

**Figure 3.** The decays on the blue end were characterized by a faster response whereas those collected at longer wavelengths were accompanied by a rise time which was due to the population flux from initially excited state to relaxed state. This trend of wavelength dependent decays is a signature of local solvation dynamics. Time-resolved emission spectra at 50 ps and 7.05 ns of C153 in HEATN are presented in **Figure 4** at two representative temperatures. The corresponding “steady-state” and “zero-time” spectra are also included. Note that unlike at 65°C, the 7.05 ns spectrum crosses the steady-state spectrum at 25°C, indicating that this spectrum does not adequately report on the completed solvation of C153, as would usually be expected for highly viscous solvents.<sup>12,70,71</sup> The spectrum recorded at 7.05 ns was red-shifted by  $\sim 270\text{ cm}^{-1}$  relative to the steady-state spectrum, demonstrating that solvation is slightly slower than the population decay of the  $S_1$  state of C153. This phenomenon has been previously observed in the case of the slowly relaxing phosphonium ionic liquids. In previous studies,<sup>12</sup> it was found that the amount of rapid solvation and the average solvation time decrease and increase, respectively, as the time-window of the experiment is increased. This phenomenon of solvation slower than the population decay of the  $S_1$  state has also been noticed elsewhere for related systems.<sup>70,71</sup> In order to compare the solvation in the ionic liquid media, we attempted to study the same in parent compound which is the neutral 4-amino-1,2,4-triazole (melting point  $\sim 85\text{ }^\circ\text{C}$ ). A solvent induced spectral shift was not observed in the molten state at  $85\text{ }^\circ\text{C}$  with the TCSPC apparatus, suggesting a very fast response for the triazole, which is consistent with its low viscosity ( $\sim 6.2\text{ cP}$ ) at the melting temperature.

The spectral shift dynamics are represented by the decay of the solvation correlation function  $C(t)$  in **Figure 5**. The  $C(t)$ s are constructed at five temperatures (25, 35, 45, 55 and  $65^\circ\text{C}$ ) and the solvation parameters are collated in **Table 4**. At all temperatures, the solvation dynamics were well described by biphasic decays, with an initial faster component preceded by a slower response. At  $25^\circ\text{C}$ , almost  $>30\%$  of the solvation is completed within instrumental time resolution ( $\sim 50\text{ps}$ ), which is

determined from the fractional solvation,  $f_{50\text{ps}}$  listed in **Table 4**. This accounts for the solvent response missed due to the finite time-resolution of the TCSPC apparatus. The missing Stokes-shift was accounted for by using the “zero-time” spectra estimated by the method of Fee and Maroncelli.<sup>69</sup> Recently Kerr-gated emission (KGE)<sup>72,73</sup> and fluorescence upconversion techniques<sup>74,75</sup> were used to measure spectral dynamics in ionic liquids with much shorter time-resolution ranging from 200 fs - 500 fs. Both the Maroncelli and Vauthey groups have reported a small but significant amount of subpicosecond component in the case of solvation in ionic liquids. Maroncelli and coworkers used a combination of KGE and TCSPC data to resolve complete solvation response in ionic liquids using 4-dimethylamino-4'-cyanostilbene (DCS) as a probe.<sup>72,73</sup> The observed response functions were well described by biphasic decays, consisting of both a sub-picosecond component of ~10-20% amplitude and a dominant slower component relaxing over a few picoseconds to several nanoseconds. The faster component was correlated to associated inertial characteristics of the constituent ions, and the slower component to solvent viscosity. The missing portion of the initial relaxation contains both subpicosecond inertial contributions as well as components relaxing on the 1-10 ps time scale<sup>73</sup> and this interpretation was also corroborated by simulations performed by Kobrak.<sup>76</sup>

As expected the solvation times decreased with increasing temperature. This was most likely because of the decrease in the viscosity of the ionic liquid allowing the neighboring solvent molecules to reorganize faster around the excited state dipole of C153. **Figure 6a** shows the dependence of solvation time on viscosity in different types of ionic liquids namely those based on imidazolium, phosphonium and triazolium cations. The solvation times of C153 in HEATN show a reasonable correlation with viscosity, whereas in imidazolium based ionic liquids the correlation is not as good; and marked deviations are observed for the phosphonium ionic liquids. This observation is consistent with those reported by Maroncelli and coworkers,<sup>71,77</sup> where they attributed the deviations in phosphonium ionic liquids to the enormous size of the cation moiety. Solvation in phosphonium ionic liquids is much slower than that of the imidazolium and HEATN systems. For example, although  $(\text{C}_6)_3\text{C}_{14}\text{P}^+ \text{Br}^-$ <sup>77</sup> is

isoviscous (~270 cP) with HEATN (at 35°C), the solvation is 5 times slower in the former. This observation can be interpreted in terms of the van der Waal volumes of the constituent ions. The radii of the cations and anions as listed in **Table 4** were estimated using Edward's<sup>78</sup> and Bondi's<sup>79</sup> van der Waal increment methods. The radii decrease in the order of phosphonium (~5.3Å) > imidazolium (~3.4Å) > triazolium (~2.9Å). This probably also explains the 2-fold faster average solvation times in HEATN compared to the isoviscous imidazolium based ionic liquids. It is noteworthy in this context that in all the imidazolium based ionic liquids studied so far, the completely relaxed state or equilibrium condition is represented adequately by the steady-state spectrum of the probe, however this was not the case in HEATN under ambient temperature.

As discussed above, besides viscosity ( $\eta$ ), the size of the individual ions strongly influences the solvent response. In order to investigate how the ion size might affect the observed solvation times, we have performed different analyses motivated by the methods of Maroncelli and coworkers,<sup>77</sup> which were used to establish correlations of the logarithm of the solvation times ( $\tau_s$ ) to various measured and calculated properties. A plot of  $\log \langle \tau_s \rangle$  versus  $\eta/T$  did not provide substantial improvement compared to a plot of  $\log \langle \tau_s \rangle$  against  $\eta$  only. Consistent with the reports of Jin et al.,<sup>77</sup> a much better correlation was found, as shown in **Figure 6b**, in which the solvation time varies as  $(\eta/T)^A R_+^B$ , where  $R_+$  is the radius of the cation, and A and B are constants determined to be 0.5 and 4.5 by multiple regression analysis. This correlation was slightly improved when the anion size ( $R_-$ ) is incorporated as shown in **Figure 6c**. Thus, the dependence of solvation time could be best described as follows:

$$\langle \tau_s \rangle \propto \sqrt{\frac{\eta/T}{R_-}} R_+^{4.5} \quad (2)$$

The diffusion times of the cation and anion of HEATN, which are the times to move a root mean square distance equal to its radius, were calculated using the relation  $t_{\pm} = \eta R_{\pm}^3 / f_{\pm} k_B T$ , where  $k_B$  is the Boltzman constant and  $f$  is 0.53 and 0.74<sup>80</sup> for '+' and '-' which refer to the cation and anion

respectively. The diffusion times are presented in **Table 4**. The correlation of solvation time with the diffusion time of the cation and anion, as shown in **Figure 7**, indicates that the contribution of the reorientational motion of ions to the overall relaxation process cannot be neglected.

### ***Rotational Dynamics of C153 in HEATN***

The fluorescence anisotropy of C153 in HEATN was measured at five different temperatures and decreased with temperature. Unlike in normal polar solvents, the anisotropy decay was non-exponential at all temperatures. The limiting anisotropy ( $r_0$ ) and rotational times are collated in **Table 4**. **Figure 8** gives the variation of rotational time ( $\tau_{rot}$ ) of C153 in HEATN as a function of temperature and viscosity in the form of  $\eta/T$ . This plot shows a good correlation in the form  $\langle \tau_{rot} \rangle \propto A(\eta/T)^{0.8}$ , where  $A$  is a constant determined from the linear fit to be 1.1. Ionic liquids have been reported to show similar correlation as established by normal polar solvents.<sup>77</sup>

The experimentally measured anisotropy decay times of C153 in HEATN have been analyzed within the framework of Stokes–Einstein–Debye (SED) hydrodynamic theory. According to this theory, the rotational diffusion of a medium sized solute molecule in a solvent continuum is assumed to occur by small step diffusion and its reorientation time and is related to the macroscopic viscosity of the solvent by the following relation<sup>81,82</sup>

$$\tau_{hyd} = \frac{V\eta}{k_B T} fC \quad (3)$$

The dashed lines in **Figure 8** are the predictions of hydrodynamic models, made by assuming C153 is of ellipsoidal shape with semi-axis dimensions of 2.0, 4.8, and 6.1 Å<sup>83</sup> and the relation where  $V$  is the solute van der Waals volume (246 Å<sup>3</sup>),  $f$  is a shape factor (1.71), and  $C$  is a “rotational coupling factor” which signifies the extent of coupling between the solute and the solvent. For stick boundary conditions  $C = 1$ , and for slip boundary conditions  $C = 0.24$ .<sup>83</sup> All of the rotation times in HEATN measured at different temperatures fall between these two limiting predictions. Deviations from the hydrodynamic predictions can be estimated from the value of the rotational coupling factor ( $C_{rot}$ ) using the relation

Distribution A: Approved for public release; distribution unlimited



$$C_{rot} = \frac{k_B T}{V \eta f} = \frac{\langle \tau_{rot} \rangle}{\tau_{stick}} \quad (4)$$

where  $\tau_{stick}$  is the stick hydrodynamic prediction. The values of  $C_{rot}$  are listed in **Table 4**. The average value in HEATN is 0.55, whereas those in conventional polar solvents were reported to be  $0.57 \pm 0.09$ .<sup>77</sup> Thus the coupling of solute and solvent between C153 and HEATN is reasonably comparable to conventional polar solvents. These results are consistent with those of Maroncelli and coworkers who reported that all ionic liquids, besides bulky ones based on phosphonium, fall within the scatter of the polar solvents.<sup>77</sup> Castner and coworkers have recently studied solvation and rotational dynamics using C153 over a range of temperatures from 5 to 80°C, in ionic liquids based on ammonium and pyrrolidinium cations. They reported small amplitudes of very long orientation relaxation time constants on the order of 100 ns, which were missing in the experiments reported on herein. All of the C153 rotational time constants in HEATN ranged from 2 – 20 ns and are in agreement with the reports by Maroncelli and coworkers.<sup>77</sup> Observation of dynamics in the time-scale of 100 ns may be unreliable where the lifetime of C153 is ~3-5 ns.

## Conclusions


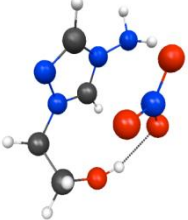
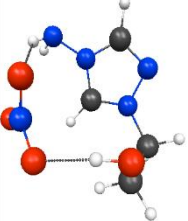
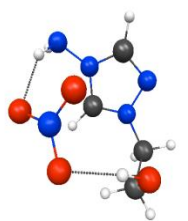
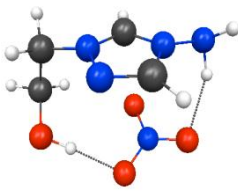
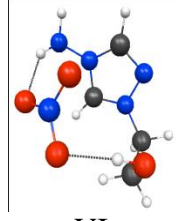
The structure and dynamics of the high-energy ionic liquid system, 1-hydroxyethyl-4-amino-1,2,4-triazolium nitrate (HEATN), were investigated. This system maintains an even charge separation assessed by both the Mulliken and geodesic derived charges. There were no instances where proton transfer was found in contrast to other reports on triazolium ionic liquids. The MP2 level optimizations find six dimer and five tetramer structures and show the significant highly hydrogen bonded network within HEATN. The FMO method adequately treats this ionic liquid system as evidenced by the small relative error obtained. Further calculations using the FMO method on this ionic liquid system are expected to give similar accuracy while using less computer resources and avoiding the prohibitive scaling of other *ab initio* methods.

Besides the structural characterization, we have undertaken a thorough temperature dependent study of solvation and rotational dynamics in HEATN using C153 as a probe and compared them with results previously obtained from earlier studies on imidazolium and phosphonium ionic liquids. The solvation time in HEATN was faster than the isoviscous imidazolium and phosphonium ionic liquids, which is probably due to the smaller size of the cationic moiety. The solvation times in HEATN showed an excellent correlation with viscosity, and the ionic radii. The fluorescence depolarization studies showed that the rotational time of C153 in HEATN at different temperatures lies within the limits of hydrodynamic predictions. The presence of the amino and hydroxyethyl groups allow HEATN to participate in significant hydrogen bonding interactions. Surprisingly, these interactions do not seem to produce a substantial difference in the dynamics of the HEATN system with respect to imidazolium systems. An exception is given in **Figure 6a**, where HEATN shows a linear correlation with a significant difference in slope compared to the imidazolium and phosphonium systems. Despite the inherent difference of having the additional nitrogen atom in the ring, no significant changes in the dynamics of this system were observed. Finally, to our knowledge this the first study of solvation dynamics in a triazolium based ionic liquid.

## **Acknowledgements**

One of the authors (TH) thanks Dr. Gregory Drake, Mr. Michael Tinnirello and Ms. Leslie Hudgens in support of material production, and funding sponsors, Dr. Michael Berman at Air Force Office of Scientific Research and Mr. Michael Huggins of the Air Force Research Laboratory.

**Table 1.** Data from dimer HEATN structures obtained via MP2.

Dimer*	$E_{\text{rel}}^{\text{a}}$ (kcal/mol)	OH-O <sup>b</sup> (Å)	NH-O <sup>b</sup> (Å)	Mulliken Charges (cation, anion) <sup>c</sup>	Geodesic Charges (cation, anion) <sup>c</sup>
 I	0	1.85	1.90	0.89, -0.89	0.82, -0.82
 II	0.6	1.84	1.96	0.83, -0.83	0.79, -0.79
 III	3.3	1.87	1.93	0.80, -0.80	0.83, -0.83
 IV	3.6	1.88	1.91	0.84, -0.84	0.80, -0.80
 V	4.0	1.84	1.93	0.83, -0.83	0.80, -0.80
 VI	5.0	1.86	1.84	0.88, -0.88	0.82, -0.82

<sup>a</sup>  $E_{\text{rel}}$  reports the energies relative to dimer “I”.

<sup>b</sup> OH-O & NH-O refer to the distance between the OH/NH group on the cation and the nearest O atom on the anion.

<sup>c</sup> Charges on each cation and anion are reported listing the cation first and the anion second for both the Mulliken charges and the geodesic charges.

\* MP2 optimized dimer structures of HEATN using the 6-31++G(d,p) basis arranged in order of increasing energy with “I” being the lowest energy structure found. The atoms are color coded such that nitrogen is represented by blue, oxygen by red, carbon by black and hydrogen by white.

**Table 2.** MP2 data of tetramer HEATN structures (see **Figure 2**)

<b>Tetramer</b>	<b>E<sub>rel</sub><sup>a</sup> (kcal/mol)</b>	<b>Ion<sup>b</sup></b>	<b>NH-O<sup>c</sup> (Å)</b>	<b>OH-N<sup>c</sup> (Å)</b>	<b>Mulliken Charge</b>	<b>Geodesic Charge</b>
<b>I</b>	<b>0.0</b>	<b>C1</b>	N/A	1.84	0.88	0.86
		<b>A1</b>			-0.88	-0.86
		<b>C2</b>	N/A	1.84	0.88	0.86
		<b>A2</b>			-0.88	-0.86
<b>II</b>	<b>10.1</b>	<b>C1</b>	1.77	1.70	0.88	0.86
		<b>A1</b>			-0.93	-0.74
		<b>C2</b>	1.73	N/A	0.92	0.78
		<b>A2</b>			-0.88	-0.91
<b>III</b>	<b>18.8</b>	<b>C1</b>	1.93	1.78	0.95	0.93
		<b>A1</b>			-0.84	-0.92
		<b>C2</b>	1.88	1.89	0.73	0.82
		<b>A2</b>			-0.84	-0.84
<b>IV</b>	<b>27.8</b>	<b>C1</b>	1.89	1.81	0.76	0.81
		<b>A1</b>			-0.77	-0.78
		<b>C2</b>	1.86	1.80	0.70	0.73
		<b>A2</b>			-0.68	-0.76
<b>V</b>	<b>39.4</b>	<b>C1</b>	N/A	1.73	0.67	0.95
		<b>A1</b>			-0.79	-0.90
		<b>C2</b>	N/A	1.75	0.94	0.83
		<b>A2</b>			-0.80	-0.88

<sup>a</sup> E<sub>rel</sub> reports the energies (kcal/mol) relative to tetramer “I”

<sup>b</sup> The ions are named as follows: the C1 ion is the ion that is perpendicular to the plane of the paper & A1 is the anion that is most closely associated with C1 (see **Figure 2**)

<sup>c</sup> OH-O & NH-O refer to the distance between the OH/NH group on the cation and the nearest O atom on the associated anion.

**Table 3.** Data obtained from evaluating the MP2 tetramer geometries (see **Figure 2**) with the FMO2-MP2 method and the FMO3-MP2 method.

Tetramer	E <sub>rel</sub> <sup>a</sup> (kcal/mol)			Ion <sup>b</sup>	FMO2-MP2		FMO3-MP2	
	MP2	FMO2-MP2 <sup>c</sup>	FMO3-MP2 <sup>d</sup>		Mulliken Charge	Geodesic Charge	Mulliken Charge	Geodesic Charge
<b>I</b>	<b>0.00</b>	<b>-0.30</b>	<b>0.02</b>	<b>C1</b>	0.90	0.93	0.87	0.83
				<b>A1</b>	-0.90	-0.93	-0.87	-0.83
				<b>C2</b>	0.90	0.94	0.87	0.83
				<b>A2</b>	-0.90	-0.93	-0.87	-0.83
<b>II</b>	<b>10.13</b>	<b>0.63</b>	<b>0.02</b>	<b>C1</b>	0.83	0.97	0.88	0.92
				<b>A1</b>	-0.87	-0.80	-0.94	-0.78
				<b>C2</b>	0.90	0.87	0.93	0.82
				<b>A2</b>	-0.86	-1.03	-0.87	-0.96
<b>III</b>	<b>18.76</b>	<b>0.55</b>	<b>-0.09</b>	<b>C1</b>	0.91	0.85	0.93	0.91
				<b>A1</b>	-0.89	-0.92	-0.85	-0.88
				<b>C2</b>	0.91	0.93	0.81	0.81
				<b>A2</b>	-0.93	-0.86	-0.89	-0.84
<b>IV</b>	<b>27.75</b>	<b>0.98</b>	<b>-0.28</b>	<b>C1</b>	0.80	0.80	0.76	0.75
				<b>A1</b>	-0.89	-0.78	-0.79	-0.73
				<b>C2</b>	0.91	0.74	0.72	0.68
				<b>A2</b>	-0.83	-0.77	-0.69	-0.71
<b>V</b>	<b>39.43</b>	<b>0.40</b>	<b>0.13</b>	<b>C1</b>	0.81	1.01	0.67	0.93
				<b>A1</b>	-0.90	-0.93	-0.77	-0.89
				<b>C2</b>	0.95	0.91	0.91	0.83
				<b>A2</b>	-0.86	-0.99	-0.82	-0.86

<sup>a</sup> E<sub>rel</sub> reports the energies (kcal/mol) relative to tetramer “I”

<sup>b</sup> The ions are named as follows: the C1 ion is the ion that is perpendicular to the plane of the paper & A1 is the anion that is most closely associated with C1 (see **Figure 2**)

<sup>c</sup> The FMO2-MP2 energy is relative to the MP2 energy for the same tetramer

<sup>d</sup> The FMO3-MP2 energy is relative to the MP2 energy for the same tetramer

**Table 4.** Solvation and anisotropy parameters in different ionic liquids.

Ionic Liquid	T (K)	$\eta^a$ (cP)	$R_+^b$ (Å)	$R_-^c$ (Å)	Anisotropy <sup>d</sup>			Solvation			
					$r_0$	$\langle\tau_{\text{rot}}\rangle$ (ns)	$C_{\text{rot}}^e$	$f_{\text{obs}}^f$	$\langle\tau_{\text{solv}}\rangle$ (ns)	$t_+$ (ns)	$t_-$ (ns)
HEATN	298	427	2.90	2.09	0.35 ±0.03	21.1 ±0.62	0.48	0.36	0.62	4.7	1.3
	308	272			0.36 ±0.10	11.3 ±0.45	0.42	0.47	0.22	2.9	0.70
	318	133			0.32 ±0.02	5.7 ±0.38	0.45	0.45	0.16	1.4	0.30
	328	69			0.38 ±0.02	4.3 ±0.68	0.67	0.53	0.10	0.7	0.18
	338	40			0.36 ±0.01	2.6 ±0.08	0.72	0.60	0.07	0.4	0.10
BMIM Cl <sup>i</sup>	343	334	3.29	2.09				0.21	0.59		
BIM NTf <sub>2</sub> <sup>i</sup>	293	90	3.16	3.39				0.65	0.20		
MIM NTf <sub>2</sub> <sup>i</sup>	293	77	2.69	3.39				0.64	0.42		
CVIM NTf <sub>2</sub> <sup>j</sup>	342	38	4.05	3.39				0.62	0.28		
P(C <sub>4</sub> ) <sub>3</sub> C <sub>16</sub> Br <sup>k</sup>	339	268	4.96	2.26				0.29	5.3		
P(C <sub>6</sub> ) <sub>3</sub> C <sub>14</sub> Cl <sup>k</sup>	331	80	5.18	2.09				0.33	3.9		

<sup>a</sup> Error bars for viscosity measurements are within ±1-2%.

<sup>b</sup> van der Waals volume of the cations ( $V_w$ ) are calculated from the Edward's atomic increments<sup>78</sup>, and the radius of ( $R_+$ ) are obtained using the relation  $R_+ = (3V_w / 4\pi)^{1/3}$

<sup>c</sup> Radius of anions ( $R_-$ ) are obtained from Bondi<sup>79</sup> and Jin et al.<sup>77</sup>

<sup>d</sup> The error bars in the anisotropy experiments are obtained from triplicate measurements.

<sup>e</sup> Rotational decoupling constant ( $C_{\text{rot}}$ ) is calculated using equation 4.

<sup>f</sup> Fractional solvation,  $f_{\text{obs}}$  are calculated at 50 ps for HEATN samples and 100 ps for other ionic liquids.

<sup>g</sup> Average solvation times,  $\langle\tau_{\text{solv}}\rangle$  are obtained by the fitting  $C(t)$  curves with two exponentials.

<sup>h</sup> The cation ( $t_+$ ) and anion( $t_-$ ) diffusion times are calculated using the equation  $t_{\pm} = \eta R_{\pm}^3 / f_{\pm} k_B T$ , where the parameters are defined in the text.

<sup>i</sup> From reference<sup>10</sup>

<sup>j</sup> From reference<sup>68</sup>

<sup>k</sup> From reference<sup>12</sup>

Distribution A: Approved for public release; distribution unlimited



## Figure captions

**Figure 1.** The structures of (a) solvatochromic probe Coumarin 153 (C153), (b) 4-amino-1,2,4-triazole, (c) 1-hydroxyethyl-4-amino-1,2,4-triazolium nitrate (HEATN), (d) 1-butyl-3-methylimidazolium chloride (BMIM<sup>+</sup> Cl<sup>-</sup>), (e) 1-butylimidazolium bis(trifluoromethylsulfonyl)imide (BIM<sup>+</sup> NTf<sub>2</sub><sup>-</sup>), (f) 1-methylimidazolium bis(trifluoromethylsulfonyl)imide (MIM<sup>+</sup> NTf<sub>2</sub><sup>-</sup>), (g) 1-cetyl-3-vinylimidazolium bromide (CVIM<sup>+</sup> Br<sup>-</sup>), (h) tetradecyl trihexyl phosphonium chloride, and (i) hexadecyl tributyl phosphonium bromide ((C<sub>4</sub>)<sub>3</sub>C<sub>16</sub>P<sup>+</sup> Br<sup>-</sup>).

**Figure 2.** Tetramer structures of HEATN obtained using the MP2 method with the 6-31++G(d,p) basis. They are labeled in order of increasing energy. In each case cation 1 is the cation that is perpendicular to the plane of the page and anion 1 is the closest corresponding anion. Red represents oxygen, blue represents nitrogen, black represents carbon and white represents hydrogen. Additional data obtained from these calculations can be seen in **Table 3**.

**Figure 3.** Representative normalized wavelength-resolved fluorescence decay traces of C153 at three different wavelengths in HEATN at 55°C. The presence of the decay and rise components as a function of wavelength is a key signature of solvation dynamics.

**Figure 4.** Time-resolved fluorescence emission spectra (TRES) of C153 in HEATN at 25°C (top panel) and 55°C (bottom panel) at 50 ps and 7.05 ns. Corresponding “steady-state” and “time-zero” spectra are also included. Note that the 7.05 ns spectra cross the “steady-state” spectrum at 25°C, indicating that these spectra do not adequately model the completed solvation of C153, as would usually be expected. The error for the steady-state and time-zero spectra is  $\sim \pm 100 \text{ cm}^{-1}$ , while for the other timed points it was  $\sim \pm 200 \text{ cm}^{-1}$ .

**Figure 5.** Solvation correlation function ( $C(t)$ ) decay curves of C153 in HEATN plotted as a function of temperature. The decays were fit with two exponentials and the average solvation time as well as the fractional solvation values can be found in **Table 4**. The typical error for each data point is  $< 0.05$ . Water content was determined to be  $< 0.3$  wt. %.

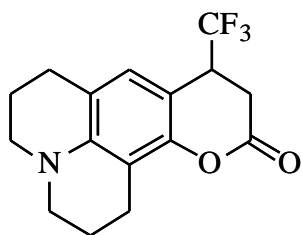
**Figure 6.** (a) The average solvation time ( $\langle\tau_s\rangle$ ) of C153 is plotted as a function of viscosity ( $\eta$ ) in different ionic liquids based namely on imidazolium, phosphonium and triazolium cations. The solvation times of C153 in HEATN show a reasonable correlation with viscosity, whereas in imidazolium and phosphonium ionic liquids studied previously poor agreement is seen. The straight line is drawn to help guide the eye. (b) Correlation of  $\langle\tau_s\rangle$  in the ionic liquids with  $\eta/T$  and cation radius ( $R_+$ ). The proportionality of  $\langle\tau_s\rangle$  varies as  $(\eta/T)^A R_+^B$ , where  $R_+$  is the radius of the cation, and A and B are constants determined to be 0.5 and 4.5 by multiple regression analysis. This correlation is slightly improved when the anion size ( $R_-$ ) is incorporated (c). These plots show a strong dependence of the solvation time on ion size. The  $R^2$  and standard deviation (SD) are obtained from the fit represented by the straight line in ‘b’ and ‘c.’

**Figure 7.** Solvation times of C153 in HEATN at five different temperatures versus estimates of the cation and anion diffusion time determined using the equation  $t_{\pm} = \eta R_{\pm}^3 / f_{\pm} k_B T$ , where the parameters are defined in the text. The linear fits are shown as solid straight lines, whereas the dashed line represents the 1:1 correlation.

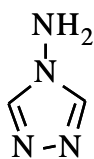
**Figure 8.** Correlation of the average rotational time ( $\langle\tau_{rot}\rangle$ ) of C153 in HEATN with viscosity ( $\eta/\text{cP}$ ) and temperature ( $T/\text{K}$ ). The solid line (red) shows the best fit of the data to the proportionality  $\langle\tau_{rot}\rangle = 1.13 \times 10^{-9} (\text{sKcP}^{-1}) (\eta/T)^{0.8}$ . The dashed lines are the average rotational times predicted from

hydrodynamic models assuming an ellipsoidal shape of C153<sup>83</sup> using “stick” and “slip” boundary conditions. The experimentally observed rotational times fall within the boundaries of hydrodynamic predictions and the deviations can be estimated by the rotational coupling factor ( $C_{\text{rot}}$ ) as described in the text.

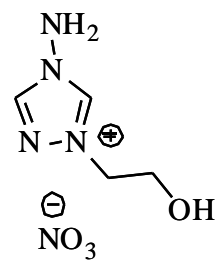
Figure 1.



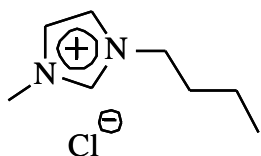
(a)



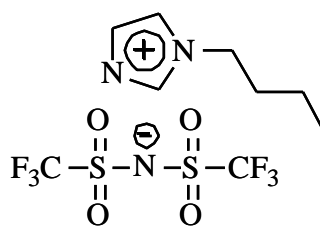
(b)



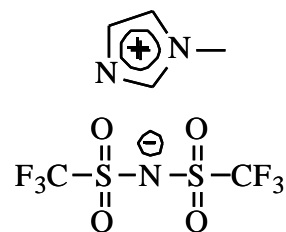
(c)



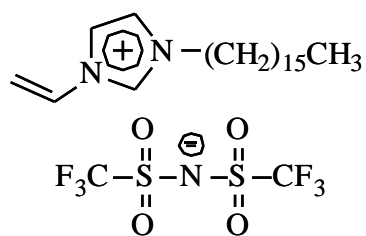
(d)



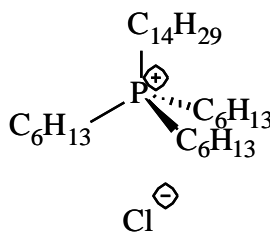
(e)



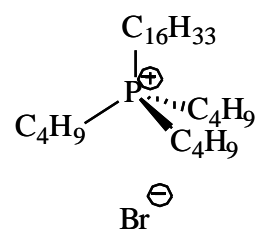
(f)



(g)



(h)



(i)

Figure 2.

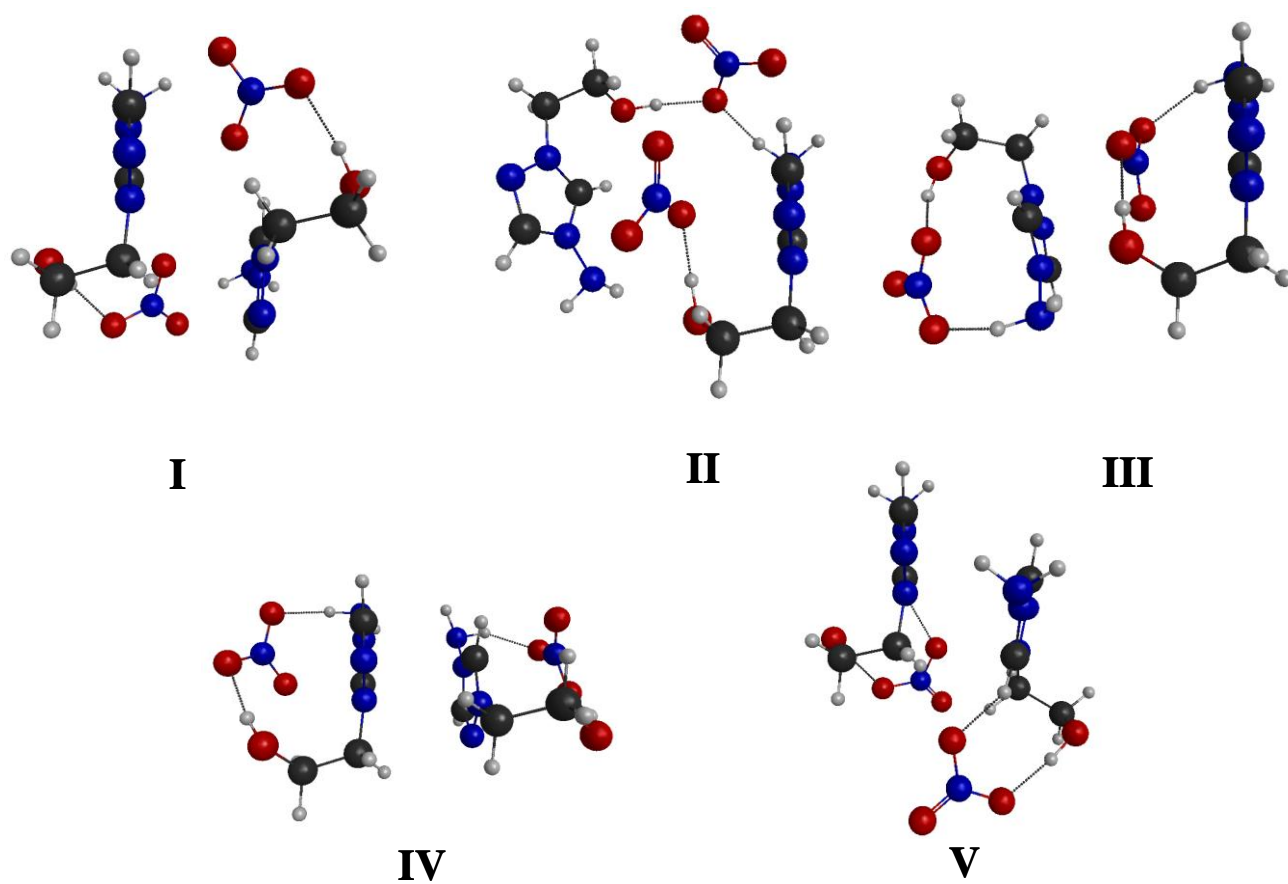


Figure 3.

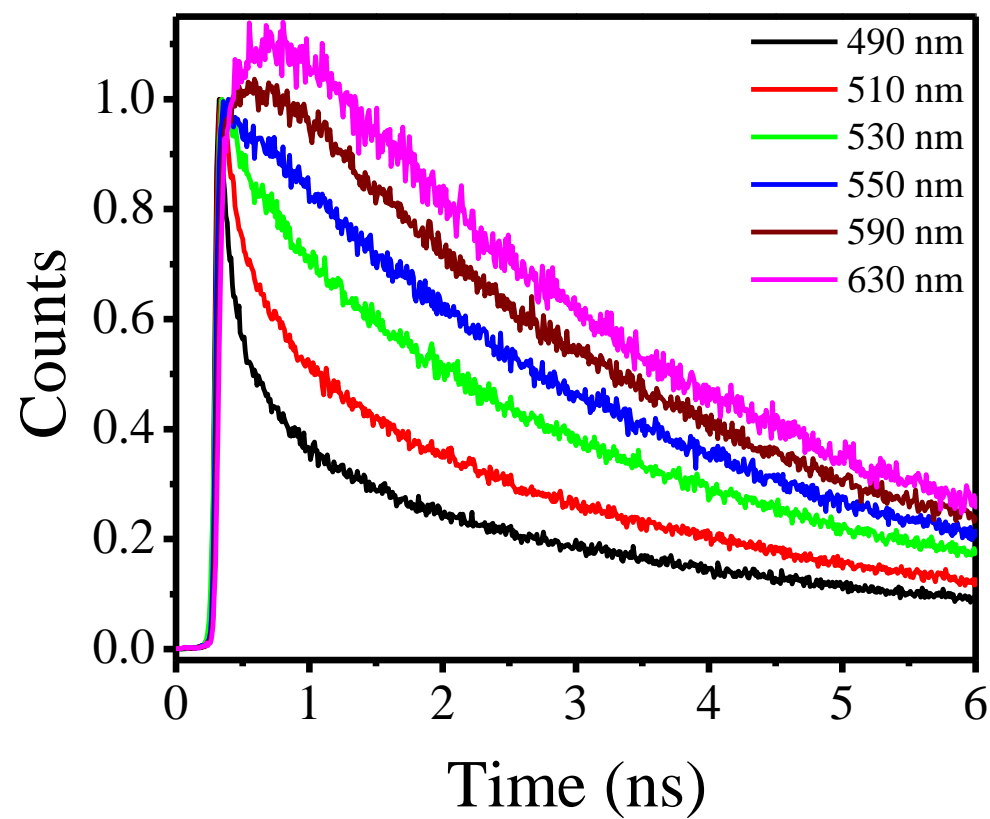


Figure 4.

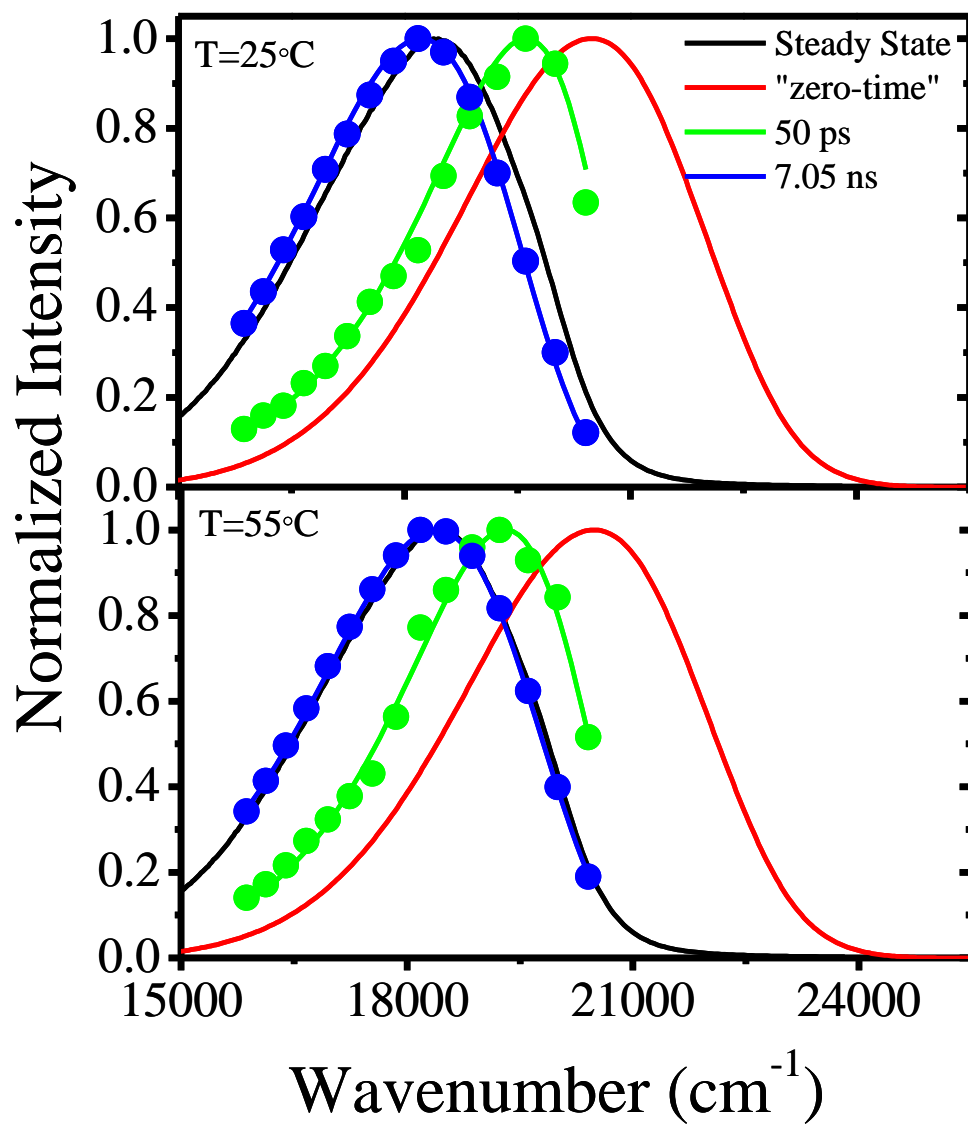
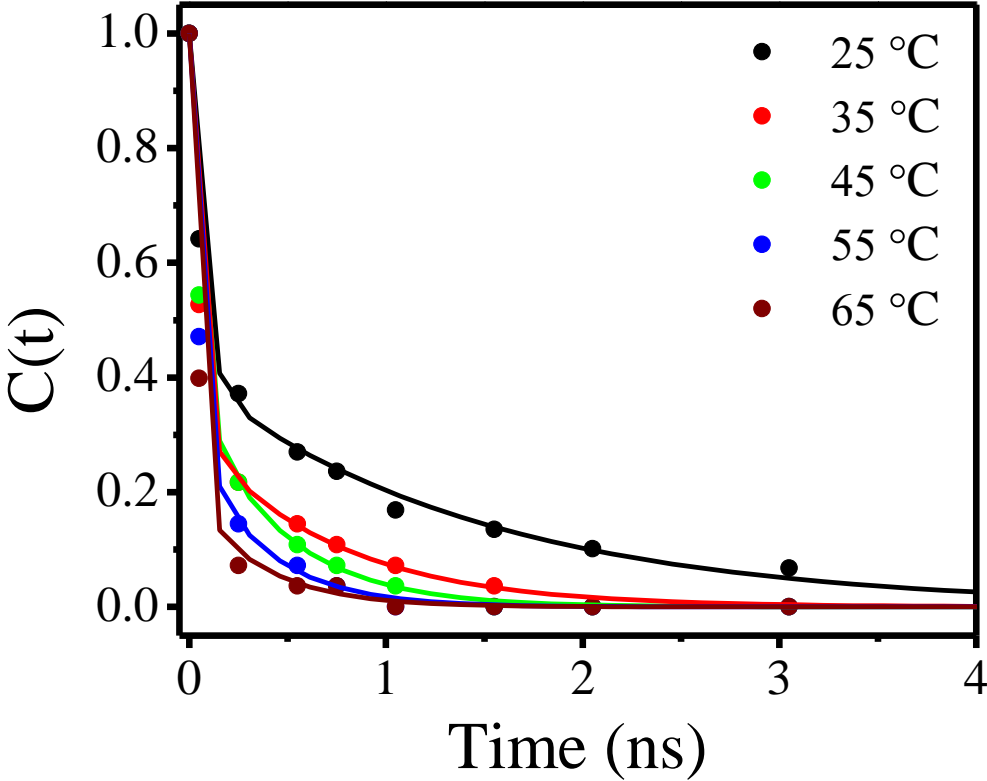


Figure 5.





Distribution A: Approved for public release; distribution unlimited

Figure 6.

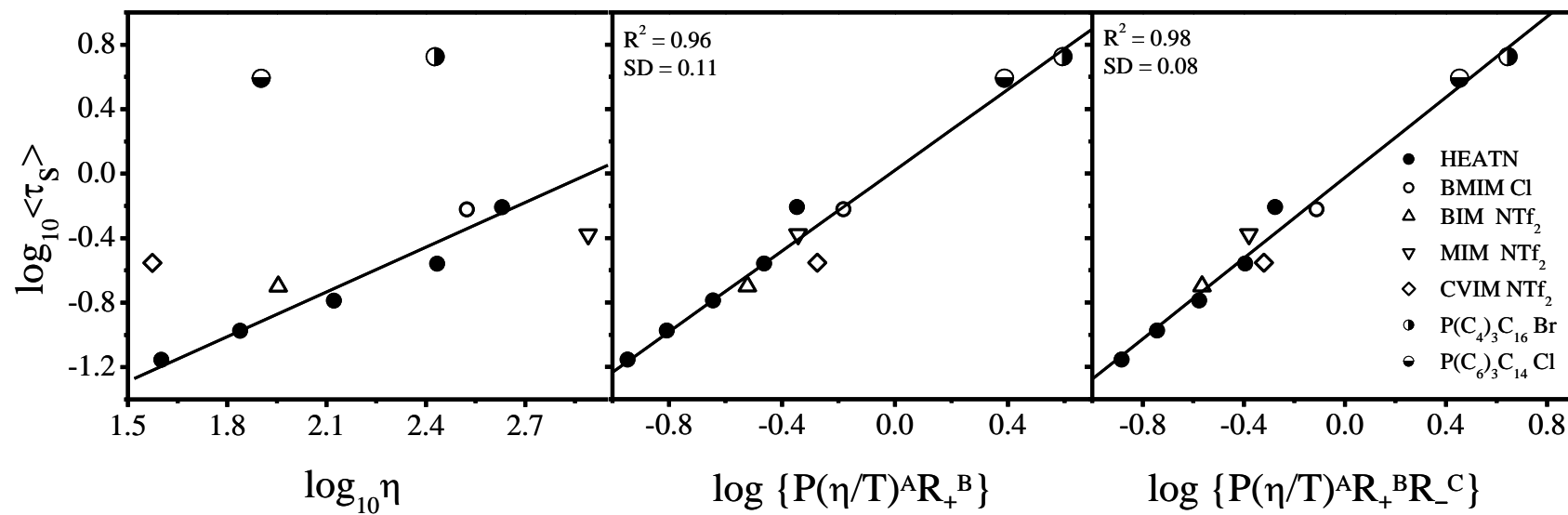


Figure 7.

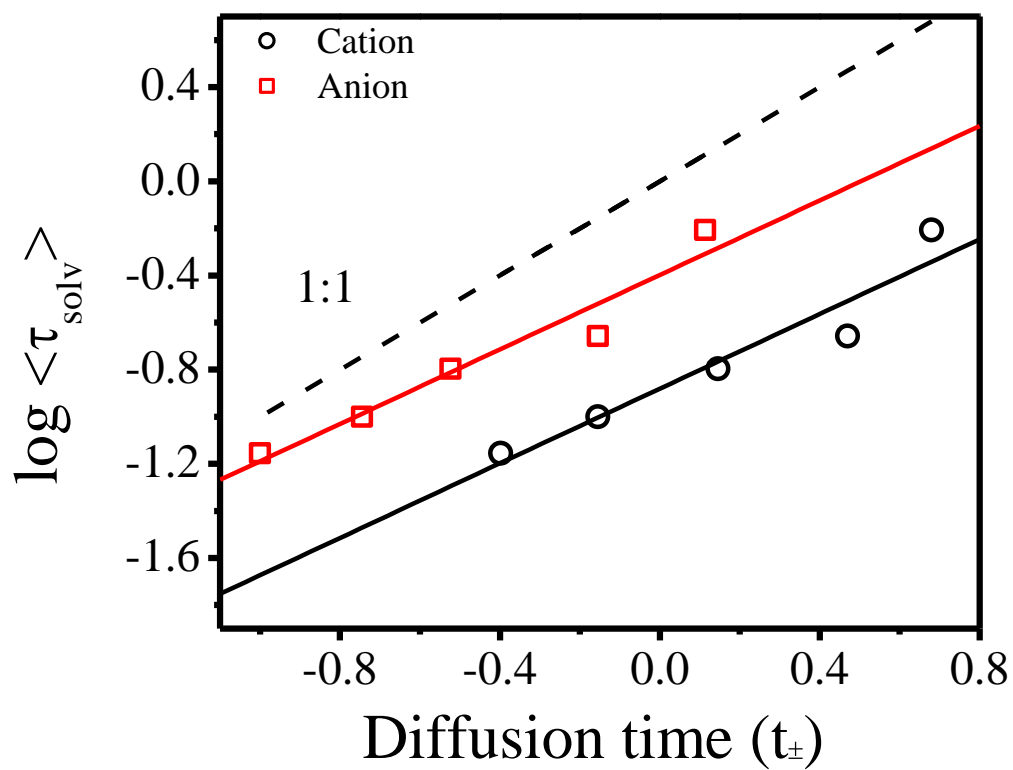
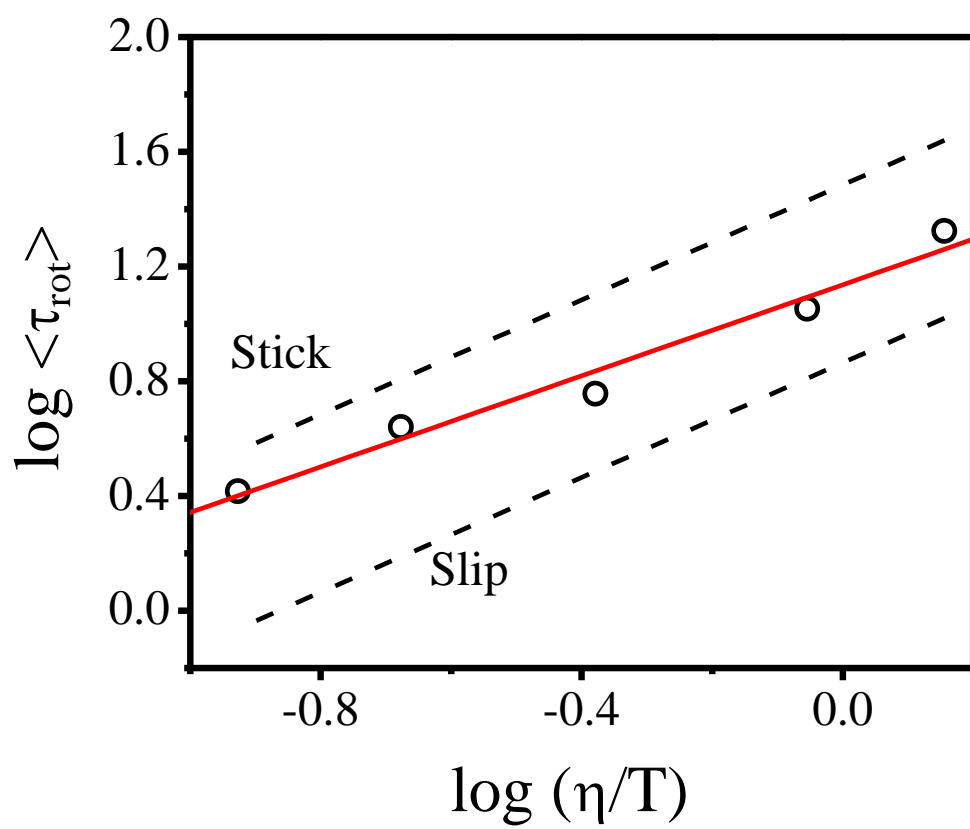


Figure 8.



## References

- (1) Deetlefs, M.; Hakala, U.; Seddon, K. R.; Wahala, K. "Ionic Liquids IV: Not just solvents anymore"; ACS 2007, Washington, D.C.
- (2) Earle, M. J.; Seddon, K. R. *Pure Appl. Chem.* **2000**, 72, 1391.
- (3) Brennecke, J. F.; Maginn, E. J. *AIChE* **2001**, 47, 2384.
- (4) Forsyth, S. A.; Pringle, J. M.; MacFarlane, D. R. *Aust. J. Chem.* **2004**, 57, 113.
- (5) Krossing, I.; Slattery, J. M.; Daguene, C.; Dyson, P. J.; Oleinikova, A.; Weingartner, H. *J. Am. Chem. Soc.* **2006**, 128, 13427.
- (6) Seddon, K. R. *Nature (Materials)* **2003**, 2, 363.
- (7) Anderson, J. L.; Ding, J.; Welton, T.; Armstrong, D. W. *J. Am. Chem. Soc.* **2002**, 124, 14247.
- (8) Welton, T. *Chem. Rev.* **1999**, 99, 2071.
- (9) Chowdhury, P. K.; Halder, M.; Sanders, L.; Calhoun, T.; Anderson, J. L.; Armstrong, D. W.; Song, X.; Petrich, J. W. *J. Phys. Chem. B* **2004**, 108, 10245.
- (10) Headley, L. S.; Mukherjee, P.; Anderson, J. L.; Ding, R.; Halder, M.; Armstrong, D. W.; Song, X.; Petrich, J. W. *J. Phys. Chem. A* **2006**, 110, 9549.
- (11) Adhikary, R.; Bose, S.; Mukherjee, P.; Thite, A.; Kraus, G. A.; Wijeratne, A. B.; Sharma, P.; Armstrong, D. W.; Petrich, J. W. *J. Phys. Chem. B* **2008**, 112, 7555.
- (12) Mukherjee, P.; Crank, J. A.; Sharma, P. S.; Wijeratne, A. B.; Adhikary, R.; Bose, S.; Armstrong, D. W.; Petrich, J. W. *J. Phys. Chem. B* **2008**, 112, 3390.
- (13) Bose, S.; Wijeratne, A. B.; Thite, A.; Kraus, G. A.; Armstrong, D. W.; Petrich, J., W. *J. Phys. Chem. B* **2009**, 113, 10825.
- (14) Hu, Z.; Margulis, C. J. *Acc. Chem. Res.* **2007**, 40, 1097.

- (15) Rogers, R. D.; Voth, G. A. *Acc. Chem. Res.* **2007**, *40*, 1077.
- (16) Fischer, G.; Holl, G.; Klapötke, T. M.; Weigand, J. J. *Thermochim. Acta* **2005**, *437*, 168.
- (17) Schmidt, M. W.; Gordon, M. S.; Boatz, J. A. *J. Phys. Chem. A* **2005**, *109*, 7285.
- (18) Zorn, D. D.; Boatz, J. A.; Gordon, M. S. *J. Phys. Chem. B* **2006**, *110*, 11110.
- (19) Pimienta, I. S. O.; Elzey, S.; Boatz, J. A.; Gordon, M. S. *J. Phys. Chem. A* **2007**, *111*, 691.
- (20) Singh, R. P.; Verma, R. D.; Meshri, D. T.; Shreeve, J. M. *Angew. Chem.* **2006**, *45*, 3584.
- (21) Drake, G.; Hawkins, T.; Brand, A.; Hall, L.; Mckay, M.; Vij, A.; Ismail, I. *Propellants, Explos., Pyrotech.* **2003**, *28*, 174.
- (22) Drake, G.; Hawkins, T.; Tollison, K.; Hall, L.; Vij, A.; Sobaski, S. “(1R)-4-Amino-1,2,4-triazolium Salts: New Families of Ionic Liquids”; ACS Symp. Ser. 902, 2005, Washington D.C.
- (23) Jiang, W.; Yan, T.; Wang, Y.; Voth, G. A. *J. Phys. Chem. B* **2008**, *112*, 3121.
- (24) Wasserscheid, P.; Keim, W. *Angew. Chem., Int. Ed.* **2000**, *39*, 3772.
- (25) Drake, G.; Hawkins, T.; Hall, L.; Boatz, J. A.; Brand, A. *Propellants, Explos., Pyrotech.* **2005**, *30*, 329.
- (26) Gordon, M. S.; Mullin, J. M.; Pruitt, S. R.; Roskop, L. B.; Slipchenko, L. V.; Boatz, J. A. *J. Phys. Chem. B* **2009**, *113*, 9646.
- (27) Fedorov, D. G.; Kitaura, K. *J. Phys. Chem. A* **2007**, *111*, 6904.
- (28) Fedorov, D. G.; Kitaura, K. Theoretical Background of the Fragment Molecular Orbital Method. In *The Fragment Molecular Orbital Method - Practical Applications to Large Molecular Systems (FMO) Method and Its Implementation in GAMESS*; Fedorov, D. G., Kitaura, K., Eds.; CRC Press, , 2009: Boca Raton, FL, 2009; pp 5.
- (29) Fedorov, D. G.; Kitaura, K. Theoretical Development of the Fragment Molecular Orbital (FMO) Method In *Modern Methods for Theoretical Physical Chemistry of Biopolymers*; Starikov, E. B., Lewis, J. P., Tanaka, S., Eds.; Elsevier: Amsterdam, 2006; pp 3.

- (30) Kitaura, K.; Ikeo, E.; Asada, T.; Nakano, T.; Uebayasi, M. *Chem. Phys. Chem. Lett.* **1999**, *313*, 701.
- (31) Nakano, T.; Kaminuma, T.; Sato, T.; Fukuzawa, K.; Akiyama, Y.; Uebayasi, M.; Kitaura, K. *Chem. Phys. Lett.* **2002**, *351*, 475.
- (32) Fedorov, D. G.; Ishida, T.; Uebayasi, M.; Kitaura, K. *J. Phys. Chem. A* **2007**, *111*, 2722.
- (33) Ishikawa, T.; Mochizuki, Y.; Nakano, T.; Amari, S.; Mori, H.; Honda, H.; Fujita, T.; Tokiwa, H.; Tanaka, S.; Komeiji, Y. *Chem. Phys. Lett.* **2006**, *427*, 159.
- (34) Maroncelli, M.; Fleming, G. R. *J. Chem. Phys.* **1987**, *86*, 6221.
- (35) Horng, M. L.; Gardecki, J. A.; Papazyan, A.; Maroncelli, M. *J. Phys. Chem.* **1995**, *99*, 17311.
- (36) Lewis, J. E.; Maroncelli, M. *Chem. Phys. Lett.* **1998**, *282*, 197.
- (37) Maroncelli, M.; Fee, R. S.; Chapman, C. F.; Fleming, G. R. *J. Phys. Chem.* **1991**, *95*, 1012.
- (38) Kovalenko, S. A.; Ruthmann, J.; Ernsting, N. P. *Chem. Phys. Lett.* **1997**, *271*, 40.
- (39) Muhlfordt, A.; Schanz, R.; Ernsting, N. P.; Farztdinov, V.; Grimme, S. *Phys. Chem. Chem. Phys.* **1999**, *1*, 3209.
- (40) Changuet-Barret, P.; Choma, C. T.; Gooding, E. F.; DeGrado, W. F.; Hochstrasser, R. M. *J. Phys. Chem. B* **2000**, *104*, 9322.
- (41) Jiang, Y.; McCarthy, P. K.; Blanchard, D. J. *Chem. Phys.* **1994**, *183*, 249.
- (42) Flory, W. C.; Blanchard, D. J. *Appl. Spectrosc.* **1998**, *52*, 82.
- (43) Palmer, P. M.; Chen, Y.; Topp, M. R. *Chem. Phys. Lett.* **2000**, *318*, 440.
- (44) Chen, Y.; Palmer, P. M.; Topp, M. R. *Int. J. Mass Spectrom* **2002**, *220*, 231.
- (45) Agmon, N. *J. Phys. Chem.* **1990**, *94*, 2959.
- (46) Chakrabarty, D.; Hazra, P.; Chakraborty, A.; Seth, D.; Sarkar, N. *Chem. Phys. Lett.* **2003**, *381*, 697.

- (47) Chowdhury, P. K.; Halder, M.; Sanders, L.; Arnold, R. A.; Liu, Y.; Armstrong, D. W.; Kundu, S.; Hargrove, M. S.; Song, X.; Petrich, J. W. *Photochem. Photobiol.* **2004**, 79, 440.
- (48) Mukherjee, P.; Halder, M.; Hargrove, M.; Petrich, J. W. *Photochem. Photobiol.* **2006**, 82, 1586.
- (49) Halder, M.; Mukherjee, P.; Bose, S.; Hargrove, M. S.; Song, X.; Petrich, J. W. *J. Chem. Phys.* **2007**, 127, 055101/1.
- (50) Bose, S.; Adhikary, R.; Mukherjee, P.; Song, X.; Petrich, J. W. *J. Phys. Chem. B* **2009**, 113, 11061.
- (51) Samanta, A. *J. Phys. Chem. Lett.* **2010**, 1, 1557.
- (52) Wishart, J. *J. Phys. Chem. Lett.* **2010**, 1, 1629.
- (53) Møller, C.; Plesset, M. S. *Phys. Rev.* **1934**, 46, 618.
- (54) Mulliken, R. S. *J. Chem. Phys.* **1955**, 23, 1833.
- (55) Mulliken, R. S. *J. Chem. Phys.* **1955**, 23, 1841.
- (56) Mulliken, R. S. *J. Chem. Phys.* **1955**, 23, 2338.
- (57) Mulliken, R. S. *J. Chem. Phys.* **1955**, 23, 2343.
- (58) Spackman, M. A. *J. Comput. Chem.* **1996**, 17, 1.
- (59) Fedorov, D. G.; Olson, R. M.; Kitaura, K.; Gordon, M. S.; Koseki, S. *J. Comput. Chem.* **2004**, 25, 872.
- (60) Fedorov, D. G.; Ishida, T.; Kitaura, K. *J. Phys. Chem. A* **2005**, 109, 2638.
- (61) Schmidt, M. W.; Baldridge, K. K.; Boatz, J. A.; Elbert, S. T.; Gordon, M. S.; Jensen, J. H.; Koseki, S.; Matsunaga, N.; Nguyen, K. A.; Su, S.; Windus, T. L.; Dupuis, M.; Montgomery, J. A., Jr. *J. Comp. Chem.* **1993**, 14, 1347.
- (62) Gordon, M. S.; Schmidt, M. W. Advances in electronic structure theory: GAMESS a decade later. In *Theory and Applications of Computational Chemistry: The First Forty Years* Dykstra, C. E., Frenking, G., Kim, K. S., Scuseria, G. E., Eds.; Elsevier Science: Amsterdam, 2005; pp 1167.
- Distribution A: Approved for public release; distribution unlimited



- (63) Bode, B. M.; Gordon, M. S. *J. Mol. Graphics Model.* **1998**, *16*, 133.
- (64) Astleford, B. A.; Goe, G. L.; Keay, J. G.; Scriven, E. F. V. *J. Org. Chem.* **1989**, *54*, 731.
- (65) Drake, G.; Hawkins, T.; Tollison, K. Energetic Ionic Salts USA, 2010; Vol. US 7745635
- (66) Earle, M. J.; Gordon, C. M.; Plechkova, N. V.; Seddon, K. R.; Welton, T. *Anal. Chem.* **2007**, *79*, 758.
- (67) Cross, A. J.; Fleming, G. R. *Biophys. J.* **1984**, *46*, 45.
- (68) Mukherjee, P.; Crank, J. A.; Halder, M.; Armstrong, D. W.; Petrich, J. W. *J. Phys. Chem. A* **2006**, *110*, 10725.
- (69) Fee, R. S.; Maroncelli, M. *Chem. Phys.* **1994**, *183*, 235.
- (70) Arzhantsev, S.; Ito, N.; Heitz, M.; Maroncelli, M. *Chem. Phys. Lett.* **2003**, *381*, 278.
- (71) Ito, N.; Arzhantsev, S.; Heitz, M.; Maroncelli, M. *J. Phys. Chem. B* **2004**, *108*, 5771.
- (72) Arzhantsev, S.; Hui, J.; Naoki, I.; Maroncelli, M. *Chem. Phys. Lett.* **2006**, *417*, 524.
- (73) Arzhantsev, S.; Jin, H.; Baker, G. A.; Maroncelli, M. *J. Phys. Chem. B* **2007**, *111*, 4978.
- (74) Lang, B.; Angulo, G.; Vauthey, E. *J. Phys. Chem. A* **2006**, *110*, 7028.
- (75) Halder, M.; Headley, L. S.; Mukherjee, P.; Song, X.; Petrich, J. W. *J. Phys. Chem. A* **2006**, *110*, 8623.
- (76) Kobrak, M. N. *J. Chem. Phys.* **2006**, Submitted.
- (77) Jin, H.; Baker, G. A.; Arzhantsev, S.; Dong, J.; Maroncelli, M. *J. Phys. Chem. B* **2007**, *111*, 7291.
- (78) Edwards, J. T. *J. Chem. Educ.* **1970**, *47*, 261.
- (79) Bondi, A. *J. Phys. Chem.* **1964**, *68*, 441.
- (80) Arzhantsev, S.; Hui, J.; Baker, G. A.; Naoki, I.; Maroncelli, M. "Solvation dynamics in ionic liquids, results from ps and fs emission spectroscopy." Femtochemistry VII, 2006.
- (81) Dutt, G. B.; Ghanty, T. K. *Journal of Chemical Physics* **2002**, *116*, 6687.
- (82) Dutt, G. B. *J. Phys. Chem. B* **2010**, *114*, 8971.

- (83) Horng, M.-L.; Gardecki, J. A.; Maroncelli, M. *J. Phys. Chem. A* **1997**, *101*, 1030.